Hyperoxia-Induced LC3B Interacts with the Fas Apoptotic Pathway in Epithelial Cell Death

Akihiko Tanaka[1,3], Yang Jin[1], Seon-Jin Lee[1], Meng Zhang[1], Hong Pyo Kim[1,4], Donna B. Stolz[2], Stefan W. Ryter[1], and Augustine M. K. Choi[1]

[1]Division of Pulmonary and Critical Care Medicine, Brigham and Women's Hospital, Harvard Medical School, Boston, Massachusetts; [2]Center for Biologic Imaging, Department of Cell Biology and Physiology, School of Medicine, University of Pittsburgh, Pittsburgh, Pennsylvania; [3]Showa University, Department of Internal Medicine, Division of Allergy and Respiratory Medicine, Tokyo, Japan; and [4]Department of Biological Sciences, College of Natural Sciences, University of Ulsan, Ulsan, Korea

Epithelial cell death plays a critical role in hyperoxia-induced lung injury. We investigated the involvement of the autophagic marker microtubule-associated protein-1 light chain-3B (LC3B) in epithelial cell apoptosis after hyperoxia. Prolonged hyperoxia (>95% O_2), which causes characteristic lung injury in mice, activated morphological and biochemical markers of autophagy. Hyperoxia induced the time-dependent expression and conversion of LC3B-I to LC3B-II in mouse lung *in vivo* and in cultured epithelial cells (Beas-2B, human bronchial epithelial cells) *in vitro*. Hyperoxia increased autophagosome formation in Beas-2B cells, as evidenced by electron microscopy and increased GFP-LC3 puncta. The augmented LC3B level after hyperoxia was transcriptionally regulated and dependent in part on the c-Jun N-terminal kinase pathway. We hypothesized that LC3B plays a regulatory role in hyperoxia-induced epithelial apoptosis. *LC3B* siRNA promoted hyperoxia-induced cell death in epithelial cells, whereas overexpression of LC3B conferred cytoprotection after hyperoxia. The autophagic protein LC3B cross-regulated the Fas apoptotic pathway by physically interacting with the components of death-inducing signaling complex. This interaction was mediated by caveolin-1 tyrosine 14, which is a known target of phosphorylation induced by hyperoxia. Taken together, hyperoxia-induced LC3B activation regulates the Fas apoptotic pathway and thus confers cytoprotection in lung epithelial cells. The interaction of LC3B and Fas pathways requires cav-1.

Keywords: apoptosis; autophagy; hyperoxia; lung injury; caveolin-1

The clinical management of severe respiratory failure may require the supplementation of mechanical ventilation with high concentrations of oxygen. However, prolonged exposure to elevated oxygen tension (hyperoxia) can cause tissue injury, particularly in the lungs. In rodents, exposure to hyperoxia triggers extensive pulmonary inflammation and degrades the alveolar–capillary barrier, leading to impaired gas exchange, and pulmonary edema (1). The pathological changes in hyperoxia-injured lungs involve the injury or death of pulmonary capillary endothelial cells and alveolar epithelial cells (2, 3).

On the basis of morphological, biochemical, and functional characteristics, cell death is classified into several major types, including necrosis and apoptosis (Type 1 programmed cell death) (4). In necrosis, an extensive cell lysis results from acute, accidental, or nonphysiological injury. In contrast, apoptosis represents a regulated form of cell death that participates in

CLINICAL RELEVANCE

Oxygen toxicity is a common complication of critical care practices involving supplemental oxygen therapy. These studies identify a protective role for autophagic proteins in hyperoxic lung cell injury, with respect to attenuating apoptotic cell death through the extrinsic pathway. This research identifies autophagy and its regulatory proteins as a potential therapeutic targets in acute lung injury.

tissue development and homeostasis, requiring the activation of proteases and nucleases within an intact plasma membrane (4). The mechanisms of hyperoxia-mediated lung cell death are complex, are cell type–specific, and remain incompletely elucidated. Previous studies have implicated apoptosis and necrosis in the mechanisms of hyperoxic lung injury and cell death in animals (5–11).

Macroautophagy, referred to herein as autophagy, is a major degradation process of organelles and cytoplasmic proteins that plays a critical role in cellular responses to metabolic stresses such as nutrient and growth factor deprivation (12–13). The molecular mechanisms of autophagy have been extensively elucidated in the past decade. During starvation, cytosol and organelles (e.g., mitochondria, endoplasmic reticulum, peroxisomes) are engulfed into double-membrane bound vesicles, called autophagosomes or autophagic vacuoles (12–13). In mammals, the conversion of microtubule-associated protein-1 light chain-3B (LC3B) from its cleaved form (LC3B-I) to LC3B-II (phosphatydylethanolamine conjugated form) is regarded as a key step in the induction of autophagosome formation (14). The outer membrane of the autophagosome fuses with lysosomes to form autolysosomes, in which the engulfed components are degraded by lysosomal hydrolases, regenerating metabolic precursors that are recycled for macromolecular synthesis and ATP generation, thereby promoting cell survival.

Autophagy serves as an adaptive or protective mechanism against cellular injury or death caused by nutrient deprivation and growth factor deprivation. However, autophagy can also promote cell death under certain circumstances (12–13). Furthermore, it has been reported that different stimuli can elicit opposite roles of autophagy with respect to cell death in the same cell type (15). Increasing evidence suggests crosstalk between apoptosis and autophagy, as several apoptosis-related factors are critically involved in autophagy (16–17). Despite growing advances in understanding the relationships between autophagy and cell death under various conditions, the regulation and specific role of autophagy in hyperoxia-induced cell death remains unknown.

Among the mechanism(s) involved in hyperoxia-induced epithelial cell apoptosis, Fas-mediated death-inducing signaling

Figure 1. Hyperoxia induces LC3B expression in mouse lung. C57BL/6 mice were exposed to room air or to hyperoxia (100% O_2) for the indicated times. (*A*) The expression of LC3B in total lung homogenates was determined by Western immunoblot analysis. Western blot is representative of $n = 2$ mice for each exposure time. β-actin served as the standard. Relative LC3B-II levels were quantified by densitometry and normalized to β-actin ($n = 5$ animals for each group). *$P < 0.01$. A time course of hyperoxia-induced LC3B was determined by Western immunoblot analysis in human lung epithelial cells (Beas2B) (*B*) and in primary human bronchial epithelial cells. (*C*) β-actin served as the standard. (*B, C*) Figures are representative of at least three independent experiments. Densitometric analyses are shown in the *bar graph*.

complex (DISC) formation plays a crucial role (18–20). Fas associates with Fas-associated death domain and caspase 8 to form the DISC complex, which triggers intrinsic and extrinsic pathways of apoptosis (21). In the current study, we demonstrate for the first time that hyperoxia induces autophagic proteins, particularly LC3B in lung epithelial cells. Furthermore, we show that hyperoxia-induced LC3B physically interacts with the Fas apoptotic pathway, providing direct evidence of the crosstalk

between apoptosis and autophagy. These data suggest an important regulatory function of LC3B in lung epithelial cells.

MATERIALS AND METHODS

The c-Jun N-terminal kinase (JNK) inhibitor SP600125 was from Calbiochem (San Diego, CA). (Anti-) Fas, Fas-associated death domain, caspase 8, cav-1, and poly-(ADP ribose) polymerase were from Santa Cruz Biotechnology (Santa Cruz, CA). Anti-LC3B was from
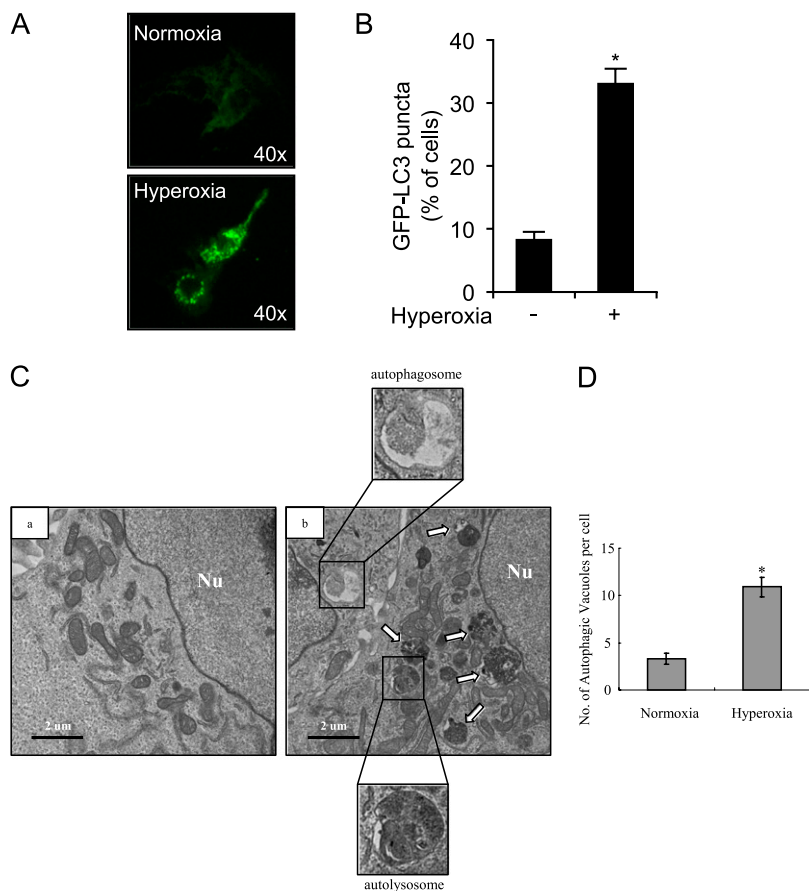
Figure 2. Hyperoxia induces autophagy in cultured epithelial cells. Beas-2B cells were transfected with 20 μg of GFP-LC3B using Lipofectamine TM2000 (Invitrogen, Carlsbad, CA) in OPTI-MEM and then exposed to normoxia or hyperoxia for 24 hours. The cells were observed under fluorescent microscopy. (*A*) Representative image is shown (original magnification: ×40). (*B*) Percentages of cells with punctuated GFP-LC3 were quantified. Results are expressed as means ± SEM of more than 100 cells per sample. Similar results were obtained from three independent experiments. *$P < 0.01$ compared with control. (*C*) The representative electron micrograph shows the ultrastructure of Beas-2B cells exposed to standard cultured conditions (normoxia) or hyperoxia for 24 hours. Representative morphology of autophagic vacuoles is shown, with evidence of autophagosome formation. Nu = nucleus; *white arrows*, autophagic vacuoles. *Scale bar*, 2 μM. (*D*) The average number of autophagic vacuoles was determined from randomly selected samples of more than 30 cells. The total numbers of autophagosomes per cell are expressed as means ± SEM. *$P < 0.01$ compared with control.
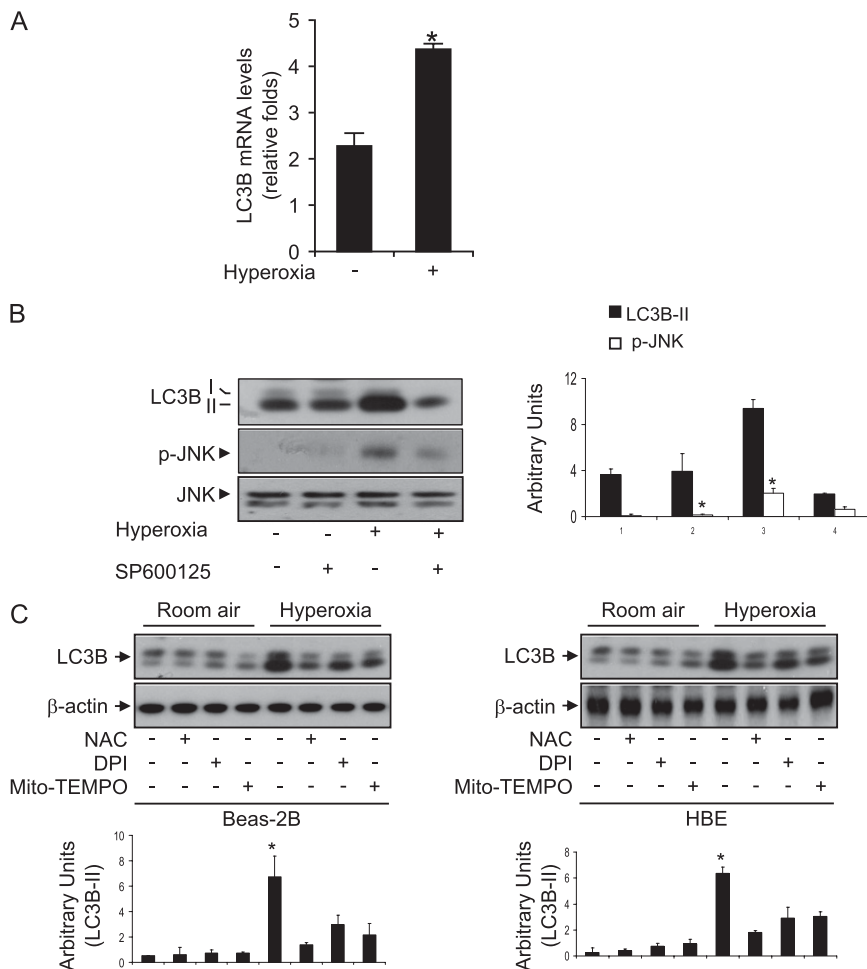
Figure 3. Involvement of c-Jun N-terminal kinase (JNK) in hyperoxia-induced autophagy. (*A*) Beas2B cells were exposed to normoxia and hyperoxia (12 h). mRNA was isolated and reverse transcribed, and Taqman real-time PCR was performed using LC3B primer and probe. Relative folds of increased mRNA transcription were displayed. (*B*) Total protein extracts (25 μg) were obtained from Beas-2B cells exposed to hyperoxia for 12 hours in the presence or absence of SP600125 (5 μM) and were subjected to immunoblot analysis with antibodies against LC3B, JNK, and phospho-JNK (pJNK). (*C*) Beas-2B cells or HBE cells were exposed to normoxia or hyperoxia for 24 hours in the presence or absence of N-acetyl-L-cysteine (NAC) (5 mM), diphenyleneiodonium (DPI) (10 μM), and mito-TEMPO (100 μM). Immunoblot analyses were performed to determine the levels of LC3B, and β-actin served as the standard. All results represent three independent experiments.

nanoTools (Teningen, Germany). Anticleaved caspase-3 was from Cell Signaling Technology (Beverly, MA). The secondary antibodies anti-rabbit IgG and anti-mouse IgG were from Santa Cruz Biotechnology.

Animal Exposures

Wild-type C57BL/6 mice (Jackson Laboratories, Bar Harbor, ME), 8 to 12 weeks of age, were maintained in laminar flow cages in a pathogen-free facility. All procedures were performed in accordance with the Council on Animal Care at the Harvard University and the National Research Council's Guide for the Humane Care and Use of Laboratory animals. The C57BL/6 mice were exposed to room air or hyperoxia (95% O_2, 5% N_2) for up to 72 hours. Lung tissue was harvested from the mice at the indicated intervals and used for biochemical analysis of autophagy.

Cell Culture and Exposure to Hyperoxia

Beas-2B cells, A549 cells, and human bronchial epithelial (HBE) 135-E6E7 cells were from American Type Culture Collection (Manassas, VA) and cultured in DMEM, F12, and keratinocyte-SFM, respectively (Invitrogen, Carlsbad, CA). Primary pulmonary epithelial cells were isolated from *cav-1*$^{-/-}$ mice (22) and wild-type mice as described (18). All media were supplemented with 10% FBS and gentamicin. Cells were maintained at 37°C in humidified incubators containing an atmosphere of 95% room air and 5% CO_2. Subconfluent cultures were used in all experiments, with the cells adhered 24 hours before the experiments. Cell cultures were exposed to hyperoxia in modular exposure chambers as described (19), using 95% O_2 with 5% CO_2. Control cells were cultured in 95% air and 5% CO_2. Cell viability was determined by Trypan blue exclusion (Invitrogen), crystal violet staining, and CellTiter-Glo

luminescent cell viability assays (Promega, Madison, WI) as described previously (16).

Western Blot

Western blot analysis for autophagic proteins was performed as previously described (23).

Electron Microscopy

Cells were fixed in 2.5% glutaraldehyde in PBS after experimental manipulations. The cells were photographed using a JEM 1210 transmission electron microscope (JEOL, Peabody, MA).

GFP-LC3 Assay

Twenty micrograms of mRFP-GFP-LC3B (a gift of Dr. Tamotsu Yoshimori) was transfected into Beas-2B cells using Lipofectamine TM2000 (Invitrogen) in OPTI-MEM for 4 hours, and then medium was replaced with complete growth medium except antibiotics. After incubation for an additional 24 hours, the cells were treated with hyperoxia for 24 hours and then fixed in 2% formaldehyde. Images were acquired with fluorescent microscopy (Leica DMLB Fluorescent Microscope: Leica Microsystems Inc., Bannockburn, IL), using the manufacturer's software (Leica QWin).

siRNA

Human LC3B and control scramble-siRNA were from Dharmacon RNAi technologies (Layfayette, CO). Beas-2B cells were incubated with siRNA at 0.1 μM using the transfection reagent and transfection medium (Santa Cruz) for 5 hours and were incubated for an additional
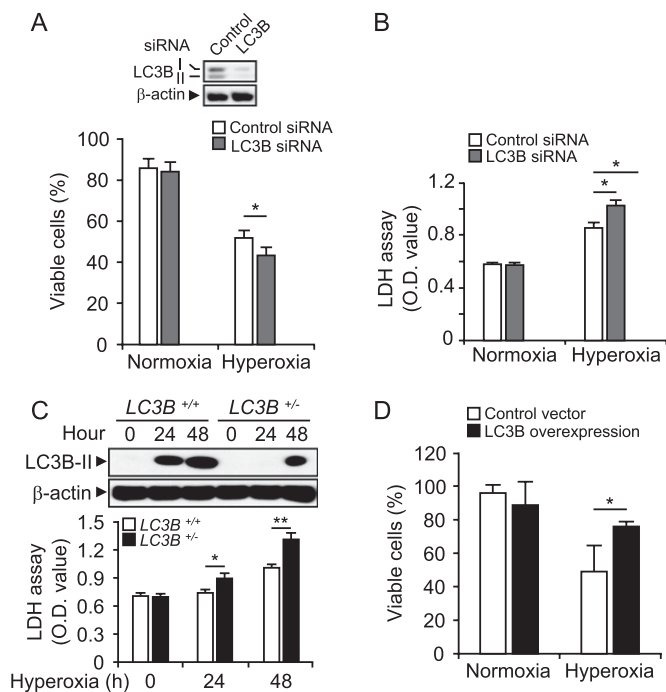
Figure 4. Cellular function of LC3B in hyperoxia-induced cell death. (*A*) Beas-2B cells were transfected with control-siRNA and LC3B-siRNA for 30 hours followed by exposure to normoxia or hyperoxia for 48 hours. Cells were labeled with FITC-Annexin V and propidium iodide (PI) and analyzed with flow cytometry (*n* = 7). Annexin V(−) and PI(−) cells were defined as live cells. The expression of LC3B was determined by Western immunoblot analysis. β-actin served as the standard (*inset*). (*B*) Cells were treated as in (*A*). Lactate dehydrogenase (LDH) levels in the supernatant were measured by Cytotoxicity Detection Kit (Roche Applied Science, Indianapolis, IN) (*n* = 8). Results are expressed as means ± SEM of indicated numbers of independent experiments. *$P < 0.05$ compared with indicated groups. Statistical significance was determined by ANOVA with multiple comparisons. (*C*) Primary lung fibroblasts were harvested from wild-type and LC3B^{+/−} mice. Equal numbers of cells (1 × 10^{6} cells per dish) were cultured on the 60-mm dishes and exposed to hyperoxia. Cells were harvested at 24 and 48 hours. (*Upper panel*) Total protein extracts (25 μg) were subjected to Western immunoblot analysis with antibodies against LC3B. (*Lower panel*) LDH levels in the supernatant were measured by Cytotoxicity Detection Kit. Results are expressed as means ± SEM of five independent experiments. *$P < 0.05$ and **$P < 0.03$ compared with indicated group. (*D*) Beas2B cells were transfected with control vector and LC3B overexpression clones. After 24 to 30 hours, cells were exposed to hyperoxia. After 48 hours, cell viability was determined. Results are expressed as means ± SEM of three independent experiments. *$P < 0.05$.

24 hours after media replacement. Transfected cells were then exposed to hyperoxia.

Lactate Dehydrogenase Release Assay

Lactate dehydrogenase (LDH) release was measured using a commercial assay (Cytotoxicity Detection Kit; Roche Applied Science, Indianapolis, IN) as previously described (19–20).

Annexin V Propidium Iodide Assay

The cells were stained with Annexin V conjugated to fluorescein and red-fluorescent propidium iodide (PI) nucleic acid–binding dye (BioVision, Mountain View, CA) according to the manufacturer's protocol and examined with a FACSCanto flow cytometer and Flow-Jo software (BD Biosciences Immunocytometry Systems, San Jose, CA).

Statistics

Data are expressed as means ± SEM, and a *P* value < 0.05 was considered significant. The significance of differences between the groups was analyzed with Student *t* test. Where appropriate, ANOVA with multiple comparisons followed by Student *t* test were used.

RESULTS

Hyperoxia Induces the Autophagic Marker LC3B

To determine the involvement of LC3B in hyperoxia-induced lung injury, we exposed mice to a hyperoxic environment (95% O_2, 5% N_2) for up to 72 hours. Hyperoxia exposure caused characteristic lung inflammation and thickening of the alveolar septa relative to normoxia-treated animals (data not shown). Hyperoxia induced a time-dependent increase in the overall expression of the autophagic marker protein LC3B in mouse lung tissue (Figure 1A).

Epithelial cells represent a primary target of hyperoxia-induced lung injury. We therefore examined the effect of hyperoxia on the activation of autophagic markers in pulmonary epithelial cells *in vitro*. Exposure of human bronchial epithelial cells (Beas-2B) to hyperoxia (95% O_2) increased total LC3B expression and LC3B-I to LCB3-II conversion after 24 hours relative to corresponding normoxic control cultures, and these levels remained elevated for up to 72 hours of exposure (Figure 1B). Increased levels of LC3B-II were also observed in primary human bronchial epithelial cells (Figure 1C) and A549 cells (data not shown) at 48 to 72 hours of exposure to hyperoxia.

Hyperoxia Induces Autophagosome Formation

Accumulation of GFP-LC3 puncta in cells transfected with GFP-LC3 is a widely accepted marker of autophagosome formation (14). Hyperoxia (24 h) caused a significant increase of GFP-LC3 puncta, representing increased autophagosome formation, in Beas-2B cells (Figures 2A and 2B).

We analyzed the ultrastructure of hyperoxia-treated cells using electron microscopic analysis. An increase of autophagic vacuoles occurred in Beas-2B cells exposed to hyperoxia for 24 hours compared with normoxic control cultures (Figures 2C and 2D). However, autophagic vacuoles almost completely disappeared in cells exposed to hyperoxia for 48 hours, which instead displayed typical necrotic features, such as swelling of mitochondria (data not shown).

Hyperoxia Up-regulates LC3B via the JNK-Mediated Pathway

We next explored the regulation of LC3B expression by hyperoxia. Hyperoxia up-regulated LC3B mRNA in Beas-2B cells as measured by Taqman real-time PCR (Figure 3A). Previous studies have shown that JNK is up-regulated by hyperoxia in mouse lung and in cultured cells and plays a major role in hyperoxia-induced cell death (24–26). To determine the specific involvement of JNK in the hypoxia-induced expression of autophagic marker protein LC3B, we first determined the effects of hyperoxia on JNK phosphorylation. As expected, hyperoxia (12 h) induced JNK phosphorylation (Figure 3B). Next, Beas-2B cells were exposed to hyperoxia in the presence or absence of the JNK inhibitor SP600125. Exposure to hyperoxia induced the phosphorylation of JNK within 12 hours (Figure 3B), with increases evident as early as 3 hours (data not shown), suggesting that phosphorylation of JNK precedes the activation of LC3B. Moreover, conversion of LC3B-I to LC3B-II in response
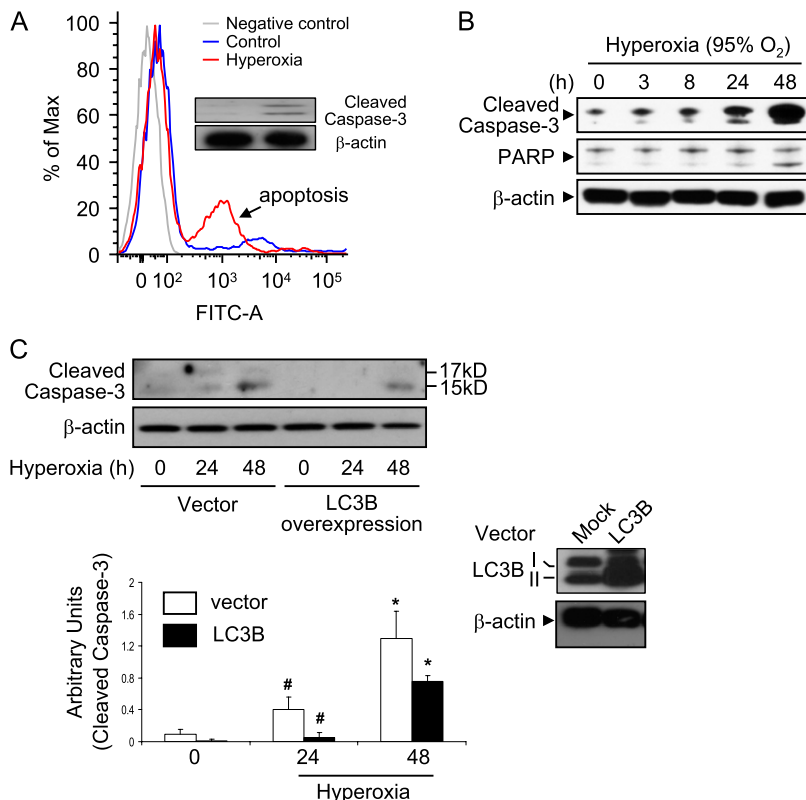
Figure 5. Effect of LC3B in hyperoxia-induced epithelial cell apoptosis. (*A*) Primary mouse lung epithelial cells were isolated from C57/BL6 mice. Cells were then exposed to room air (RA) or hyperoxia (24 h). Annexin V and PI were used to stain cells, and fluorescence-activated cell sorter analysis was performed. *Inset*: Cleaved caspase 3 was determined using Western blot analysis. (*B*) Beas-2B cells were exposed to hyperoxia for up to 48 hours and harvested at the indicated times. Total protein extracts (25 μg) were subjected to immunoblot analysis with antibodies against the cleaved form of caspase-3 (c-caspase-3) or poly-(ADP ribose) polymerase (PARP). β-actin served as the standard. (*C*) Beas-2B cells were transfected with control vectors or LC3B overexpression clones. After 24 hours, cells were exposed to hyperoxia (24 and 48 h). Hyperoxia-induced cleaved caspase 3 (active form) was determined using Western blot analysis. Overexpression of LC3B was confirmed by protein level determined using Western blot analysis (*inset*). All results represent three independent experiments.

to hyperoxia was suppressed by the treatment of epithelial cells with the JNK inhibitor SP600125 (Figure 3B).

To determine whether hyperoxia induced LC3B activation via reactive oxygen species (ROS), Beas-2B cells were pretreated with the ROS inhibitor N-acetyl-L-cysteine (NAC), the NAD(P)H oxidase inhibitor diphenyleneiodonium, or the mitochondrial antioxidant MitoTEMPO followed by hyperoxia. LC3B expression was evaluated using Western blot analysis. We found that NAC, diphenyleneiodonium, and MitoTEMPO inhibited hyperoxia-induced LC3B expression in Beas2B and HBE cells (Fig. 3C).

Cellular Function of LC3B in Hyperoxia-Induced Cell Death

To address the role of LC3B in hyperoxia-induced cell death, Beas-2B cells were transfected with siRNA targeting *LC3B* and then exposed to hyperoxia. The effectiveness of siRNA treatment is shown in Figure 4A (*inset*). Next, we explored the effect of transfection with *LC3B* siRNA on cell viability assessed by Annexin V/PI staining using flow cytometry and on LDH release. Annexin V(−)/ PI(−) cells are considered as live cells. The *LC3B* siRNA did not affect the percentage of live cells or LDH release under normoxic conditions (Figures 4A and 4B). On the other hand, *LC3B* siRNA reduced viability and increased LDH release under hyperoxic conditions, compared with that in control siRNA-transfected cells (Figures 4A and 4B). We also examined the effect of LC3B in hyperoxia using *LC3B*$^{+/-}$ murine primary fibroblast cells (27). The expression level of LC3B-II was increased by hyperoxia in *LC3B*$^{+/-}$ fibroblasts. As expected, the magnitude of LC3B-II expression in response to hyperoxia in *LC3B*$^{+/-}$ cells was lower than that in wild-type cells (Figure 4C). Consistent with the effect of transfection with *LC3B*-siRNA, inherent down-regulation of LC3B in these cells contributed to hyperoxia sensitivity, as demonstrated by increased LDH release (Figure 4C). To confirm our observation using a "gain-of-

function" approach, we overexpressed LC3B in Beas-2B cells. After hyperoxia (48 h), cell viability was determined as described in MATERIALS AND METHODS. We found that LC3B-overexpressing cells were more resistant to hyperoxia-induced cell death compared with cells transfected with empty vector (Figure 4D). These data, taken together, suggest that LC3B confers partial cytoprotection against hyperoxia-induced cell death in lung epithelial cells.

LC3B Interacts with Apoptotic Pathways in Hyperoxia-Induced Cell Death

We examined the mechanisms of hyperoxia-induced cell killing in epithelial cells. We first determined whether hyperoxia induces lung epithelial cell apoptosis using primary lung epithelial cells isolated from C57/BL6 mice. Primary lung epithelial cells underwent apoptosis after 12 hours of hyperoxia exposure, consistent with previous reports (18) (Figure 5A). Furthermore, hyperoxia induced the expression of the cleaved (active) form of caspase 3 in lung epithelial cells (Figure 5A, *inset*), suggesting that caspase-dependent apoptosis is critically involved in hyperoxia-induced lung epithelial cell death. Consistently, hyperoxia caused an early activation of apoptosis by 24 hours of exposure in Beas-2B cells, associated with loss of cell viability as determined by caspase-3 cleavage, poly-(ADP ribose) polymerase activation (Figure 5B), and Trypan Blue exclusion (data not shown). LDH release, a marker of necrotic cell death, appeared after 48 hours continuous exposure, consistent with morphological features of necrosis, such as dilation of cytoplasmic organelles, which were evident under electron microscopy at 48 hours (data not shown). To confirm that LC3B plays a role in hyperoxia-induced apoptosis, we overexpressed LC3B in Beas-2B cells. Overexpression of LC3B decreased hyperoxia-induced cleavage of caspase 3 compared with cells transfected with empty vector (mock transfection) (Figure 5C). The overexpression of
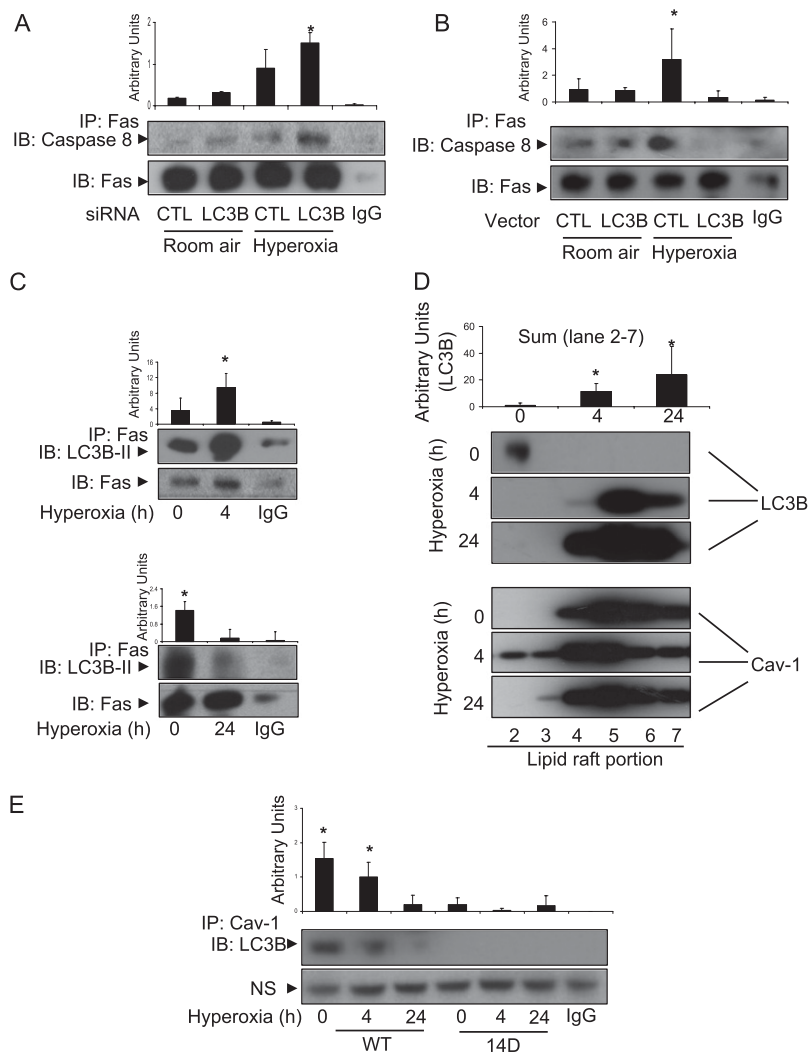
Figure 6. Crosstalk of autophagy with apoptosis. (*A*) Beas-2B cells were transfected with control siRNA or LC3B siRNA. After 24 hours, cells were exposed to hyperoxia (4 h). Co-IP assays were performed to detect the interaction between Fas and caspase 8. (*B*) Beas-2B cells were transfected with control vector or LC3B expression vector. After 24 hours of transfection, cells were exposed to hyperoxia (4 h). Co-IP assays were performed to detect the interaction between Fas and caspase 8. (*C*) Beas2B cells were exposed to normoxia or hyperoxia for 4 hours (*upper panels*) and 24 hours (*lower panels*). The interaction between Fas and LC3B was determined by co-IP assays. (*D*) Beas2B cells were exposed to normoxia or hyperoxia for 4 hours. Lipid rafts were isolated, and the amount of LC3B trafficking into the lipid raft fraction was determined using Western blot analysis. (*E*) Beas2B cells were transfected with caveolin-1 wild-type Y14 clone and Y14D (tyrosine to aspartate) mutant clones. Cells were then exposed to hyperoxia (24 or 48 h). LC3B and cav-1 interaction was determined using co-IP assays and Western blot analysis. NS = nonspecific binding. Results are representative of three independent experiments.

LC3B was confirmed by Western blot analysis (Figure 5C, *inset*). Knocking down LC3B using siRNA resulted in an up-regulation of cleaved caspase 3 (data not shown).

To investigate the interrelationships between LC3B and apoptotic pathway components in hyperoxia-induced cell death, we determined the effect of LC3B on hyperoxia-induced DISC formation. Treatment with LC3B siRNA induced DISC formation during hyperoxia, as detected by Fas-caspase 8 interaction using co-IP assays (Figure 6A). Overexpression of LC3B decreased the Fas-caspase 8 interaction after hyperoxia (Figure 6B), suggesting that LC3B interacted with the Fas-DISC–dependent apoptotic pathways. Next, we found that LC3B and Fas interacted physically by co-IP assays. This interaction was augmented after 4 hours of hyperoxia exposure (Figure 6C, *upper panel*). However, prolonged exposure to hyperoxia resulted in dissociation of the complex of LC3B and Fas (Figure 6C, *lower panel*). A previous report has shown that Fas-DISC formation occurs within the lipid rafts and caveolae (18). To determine the cellular location where LC3B interacts with Fas, we first examined LC3B trafficking after hyperoxia. Hyperoxia induced LC3B trafficking into the lipid rafts after 4 hours of hyperoxia exposure (Figure 6D). This result is consistent with our previous findings that cav-1, a caveolae/lipid raft marker protein, is required for LC3B and Fas interaction (28). The interaction between Fas and LC3B was abolished in cav-1 null cells (data not shown). Prolonged hyperoxia (24 h) interrupted the associations

between LC3B and cav-1 (Figure 6E), suggesting that prolonged hyperoxia may abolish the protective effects of LC3B. Furthermore, transfecting Beas-2B cells with cav-1 Y14 (tyrosine 14) mutant Y14D (tyrosine to aspartic acid) abolished the interactions between cav-1 and LC3B. This result suggests that Y14 is crucial for the LC3B–cav-1 interaction.

DISCUSSION

In this study, we have observed increased markers of autophagy (i.e., LC3B activation) in the lungs of C57BL/6 mice and in cultured epithelial cells subjected to experimental hyperoxia, suggestive of an inducible adaptive mechanism. Hyperoxia was found to induce the expression and activation of the autophagic protein LC3B and to stimulate autophagosome formation, two hallmarks of autophagic pathway initiation. Prolonged exposure to hyperoxia caused time-dependent cell death associated with the activation of caspase-3. We have therefore explored the relationships between the autophagic marker protein LC3B and cell death pathways in epithelial cells exposed to hyperoxia.

Although apoptosis, necrosis, and autophagy are delineated by distinct histological characteristics and underlying signaling pathways, these different phenotypes of cell death are often activated simultaneously or sequentially by the same stimuli, stress, or pharmacological intervention *in vivo* and *in vitro*. Hyperoxia-induced epithelial cell death has been shown to involve elements
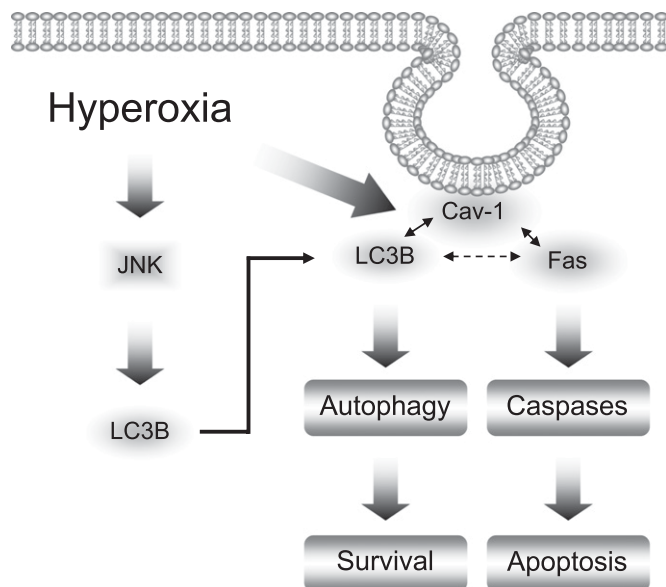
Figure 7. Schemata of proposed pathways. Autophagy promotes cell survival after hyperoxia via interacting with Fas-mediated apoptosis pathways. Hyperoxia induces LC3B expression, a key initiator of autophagy. In this study, we describe dynamic interactions between LC3B and the apoptotic regulator Fas. Forced expression of LC3B was found to diminish apoptotic pathway initiation by the Fas-dependent death-inducing signaling complex. The interactions of LC3B and Fas are dependent on caveolin-1 and its phosphorylation state at Y-14. The balance between LC3B/cav-1/Fas complex determines the fate of the cell.

of apoptosis and necrosis, with potential overlap between the two pathways (5–11, 19). Previous studies have indicated that hyperoxia primarily induces necrosis in A549, MLE12, type I epithelial cells, and murine lung bronchial cells (5–6). Our recent studies demonstrate concurrent activation of the apoptogenic caspase-8/Bid pathway in hyperoxia-treated A549 cells, suggestive of a mixed cell death phenotype (19). Studies in alveolar macrophages and pulmonary endothelial cells indicate apoptosis as a primary mechanism with activation of caspases (11, 19–20). Thus, apoptosis signaling pathways may play an important role in hyperoxia-induced lung cell death regardless of whether the final phenotypic outcome resembles apoptosis or necrosis (19).

Consistent with a major role for excessive ROS production in oxygen toxicity, we have found that the increased expression and conversion of LC3B induced by hyperoxia is mediated largely via induction of ROS production. This conclusion is supported by attenuation of the response by the general antioxidant NAC. Furthermore, inhibitors of NADPH oxidase and targeted inhibitors of mitochondrial ROS production also partially attenuate the response, suggesting that ROS generation from cytosolic and mitochondrial sources may be involved.

In the present study, we have shown that the autophagy marker protein LC3B directly interacts with the apoptotic signaling molecule Fas after hyperoxic exposure (4 h). We identify this event as cytoprotective because forced overexpression of LC3B attenuates Fas-related DISC formation in response to hyperoxia at early time points. Hyperoxia exposure (4 h) further increased the association of LC3B with Fas. At later time points (i.e., 24 h), prolonged hyperoxia led to the dissociation of this complex (data not shown). This result suggests that prolonged hyperoxia, unlike short-term exposure, interrupts the LC3B/Fas interaction and abolishes the protective effects of LC3B during hyperoxia-induced cell death (Figure 7). The current results indicate that apoptosis, in particular an extrinsic signaling pathway mediated

by DISC and caspase-8, may be regulated by autophagy during hyperoxia-induced cell death. These results are in contrast with our previous findings in a cigarette smoke model showing that treatment of epithelial cells with cigarette smoke extract caused rapid dissociation of the LC3B-Fas complexes (28). These differences may reflect differential effects of cellular stress stimuli with respect to kinetic profiles. The observations may reflect the fact that cigarette smoke extract exposure represents a much faster acting model of acute toxicity. With later kinetic time points (i.e., 24 h hyperoxia), the dissociation of LC3B from Fas mimics that observed with short-term exposure to cigarette smoke (1–2 h). Thus, the functional role of autophagic proteins such as LC3B in hyperoxia-induced cell death may be contingent on the duration and strength of stress signals and on other regulators involved in cellular homeostasis.

The modest but statistically significant effects of LC3B modulation on cell survival indicate that LC3B plays a partial role in cell survival signaling after hyperoxia. Although we report novel interactions of LC3B with Fas and cav-1, we cannot exclude the possibility that other LC3B-interacting proteins may contribute to the phenotypic observations. In particular, $p62^{SQSTM1}$ has been recently described as a binding partner for LC3B, which facilitates the autophagosomal degradation of ubiquitinated proteins. Further experiments examining the role of $p62^{SQSTM1}$ in hyperoxic cell death may be warranted (29).

Consistent with our previous report (28), cav-1 is required to facilitate the interaction between Fas and LC3B. In addition to the cav-1 CSD domain (28), we found that cav-1 Y14 tyrosine is critical for the association of LC3B with cav-1. Previous reports show that hyperoxia triggers cellular signaling via modifying cav-1 phosphorylation on Y14 (18). Hyperoxia caused the time-dependent decrease of the association between cav-1 and LC3B, whereas the Y14D mutation abolished LC3B-cav1 interaction. The initial and late effects of hyperoxia on LC3B/cav-1/Fas complex formation may be mediated via different motifs, such as cav-1 Y14 or cav-1 CSD.

Due to the apparent increases in autophagosome formation after hyperoxic exposure, it remains likely that the process of autophagy may exert a prosurvival role in hyperoxic exposure. In general, autophagy at basal levels plays an important role to retain cellular homeostasis; meanwhile, insufficient and excessive autophagy is considered to be harmful for cells and may result in cell death (30). We conclude that the hyperoxia-induced autophagic protein LC3B has a protective role against cell death, probably in the initial phase after hyperoxia, by directly interacting with and inhibiting Fas/DISC-dependent apoptotic pathways. We cannot exclude the possibility that the effects of LC3B in this model represent signaling sequelae independent of the role of this protein in facilitating autophagosome formation and initiating the autophagic pathway. Thus, further experiments with inhibitors of autophagic flux, including inhibitors of lysosomal processing and autophagosome/lysosome fusion, may elucidate these relationships.

Prior studies have shown that the inhibition of JNK may promote cell survival *in vitro* (24–25). On the other hand, JNK1-deficient mice were more susceptible to hyperoxia than wild-type mice (26), indicating the multifunctional role of JNK in hyperoxia-induced lung injury. In this study, we found that JNK regulates the hyperoxia-mediated induction of the autophagy marker protein LC3B, which represents a novel function of JNK in hyperoxia-induced cell injury. JNK has been shown to regulate autophagy induced by other stimuli, such as starvation, ER stress, T-cell receptor activation, and cytokine stimulation (31–33), regardless of whether autophagy was implicated in the protection or promotion of cell death. The mechanisms by which JNK regulate autophagy remain unclear.

In conclusion, autophagic protein LC3B, under the regulation of stress-inducible signaling cascades, may play critical roles in maintaining cellular homeostasis and cytoprotection during oxidative stress. Manipulation of autophagic pathways may provide additional therapeutic targets in the management of acute lung injury.

References

1. Crapo JD. Morphologic changes in pulmonary oxygen toxicity. _Annu Rev Physiol_ 1986;48:721–731.
2. Mantell LL, Lee PJ. Signal transduction pathways in hyperoxia-induced lung cell death. _Mol Genet Metab_ 2000;71:359–370.
3. Crapo JD, Barry BE, Foscue HA, Shelburne J. Structural and biochemical changes in rat lungs occurring during exposures to lethal and adaptive doses of oxygen. _Am Rev Respir Dis_ 1980;122:123–143.
4. Galluzzi L, Maiuri MC, Vitale I, Zischka H, Castedo M, Zitvogel L, Kroemer G. Cell death modalities: classification and pathophysiological implications. _Cell Death Differ_ 2007;14:1237–1243.
5. Barazzone C, Horowitz S, Donati YR, Rodriguez I, Piguet PF. Oxygen toxicity in mouse lung: pathways to cell death. _Am J Respir Cell Mol Biol_ 1998;19:573–581.
6. Kazzaz JA, Xu J, Palaia TA, Mantell L, Fein AM, Horowitz S. Cellular oxygen toxicity: oxidant injury without apoptosis. _J Biol Chem_ 1996; 271:15182–15186.
7. O'Reilly MA, Staversky RJ, Watkins RH, Reed CK, de Mesy Jensen KL, Finkelstein JN, Keng PC. The cyclin-dependent kinase inhibitor p21 protects the lung from oxidative stress. _Am J Respir Cell Mol Biol_ 2001;24:703–710.
8. De Paepe ME, Mao Q, Chao Y, Powell JL, Rubin LP, Sharma S. Hyperoxia-induced apoptosis and Fas/FasL expression in lung epithelial cells. _Am J Physiol Lung Cell Mol Physiol_ 2005;289:L647–L659.
9. Pagano A, Pitteloud C, Reverdin C, Métrailler-Ruchonnet I, Donati Y, Barazzone Argiroffo C. Poly(ADP-ribose)polymerase activation mediates lung epithelial cell death in vitro but is not essential in hyperoxia-induced lung injury. _Am J Respir Cell Mol Biol_ 2005;33:555–564.
10. McGrath-Morrow SA, Stahl J. Apoptosis in neonatal murine lung exposed to hyperoxia. _Am J Respir Cell Mol Biol_ 2001;25:150–155.
11. Petrache I, Choi ME, Otterbein LE, Chin BY, Mantell LL, Horowitz S, Choi AM. Mitogen-activated protein kinase pathway mediates hyperoxia-induced apoptosis in cultured macrophage cells. _Am J Physiol_ 1999;277:L589–L595.
12. Mizushima N, Levine B, Cuervo AM, Klionsky DJ. Autophagy fights disease through cellular self-digestion. _Nature_ 2008;451:1069–1075.
13. Ravikumar B, Sarkar S, Davies JE, Futter M, Garcia-Arencibia M, Green-Thompson ZW, Jimenez-Sanchez M, Korolchuk VI, Lichtenberg M, Luo S, et al. Regulation of mammalian autophagy in physiology and pathophysiology. _Physiol Rev_ 90:2010;1383–1435.
14. Klionsky D, Abeliovich H, Agostinis P, Agrawal DK, Aliev G, Askew DS, Baba M, Baehrecke EH, Bahr BA, Ballabio A, et al. Guidelines for the use and interpretation of assays for monitoring autophagy in higher eukaryotes. _Autophagy_ 2008;4:151–175.
15. Wang Y, Singh R, Massey AC, Kane SS, Kaushik S, Grant T, Xiang Y, Cuervo AM, Czaja MJ. Loss of macroautophagy promotes or prevents fibroblast apoptosis depending on the death stimulus. _J Biol Chem_ 2008;283:4766–4777.
16. Pattingre S, Tassa A, Qu X, Garuti R, Liang XH, Mizushima N, Packer M, Schneider MD, Levine B. Bcl-2 antiapoptotic proteins inhibit Beclin 1-dependent autophagy. _Cell_ 2005;122:927–939.

17. Crighton D, Wilkinson S, O'Prey J, Syed N, Smith P, Harrison PR, Gasco M, Garrone O, Crook T, Ryan KM. DRAM, a p53-induced modulator of autophagy, is critical for apoptosis. _Cell_ 2006;126:121–134.
18. Zhang M, Lee SJ, An C, Xu JF, Joshi B, Nabi IR, Choi AM, Jin Y. Caveolin-1 mediates Fas-BID signaling in hyperoxia-induced apoptosis. _Free Radic Biol Med_ 2011;50:1252–1262.
19. Wang X, Ryter SW, Dai C, Tang Z, Watkins SC, Yin X, Song R, Choi AM. Necrotic cell death in response to oxidant stress involves the activation of the apoptogenic caspase-8/Bid pathway. _J Biol Chem_ 2003;278:29184–29191.
20. Wang X, Wang Y, Kim HP, Nakahira K, Ryter SW, Choi AM. Carbon monoxide protects against hyperoxia-induced endothelial cell apoptosis by inhibiting reactive oxygen species formation. _J Biol Chem_ 2007;282:1718–1726.
21. Peter ME, Krammer PH. The CD95(APO-1/Fas) DISC and beyond. _Cell Death Differ_ 2003;10:26–35.
22. Drab M, Verkade P, Elger M, Kasper M, Lohn M, Lauterbach B, Menne J, Lindschau C, Mende F, Luft FC, et al. Loss of caveolae, vascular dysfunction, and pulmonary defects in caveolin-1 gene-disrupted mice. _Science_ 2001;293:2449–2452.
23. Chen Z-H, Kim HP, Sciurba FC, Lee S-J, Feghali-Bostwick C, Stolz DB, Dhir R, Landreneau RJ, Schuchert MJ, Yousem SA, et al. Egr-1 regulates autophagy in cigarette smoke-induced chronic obstructive pulmonary disease. _Plos One_ 2008;3:e3316.
24. Romashko J III, Horowitz S, Franek WR, Palaia T, Miller EJ, Lin A, Birrer MJ, Scott W, Mantell LL. MAPK pathways mediate hyperoxia-induced oncotic cell death in lung epithelial cells. _Free Radic Biol Med_ 2003;35:978–993.
25. Li Y, Arita Y, Koo HC, Davis JM, Kazzaz JA. Inhibition of c-Jun N-terminal kinase pathway improves cell viability in response to oxidant injury. _Am J Respir Cell Mol Biol_ 2003;29:779–783.
26. Morse D, Otterbein LE, Watkins S, Alber S, Zhou Z, Flavell RA, Davis RJ, Choi AM. Deficiency in the c-Jun NH2-terminal kinase signaling pathway confers susceptibility to hyperoxic lung injury in mice. _Am J Physiol Lung Cell Mol Physiol_ 2003;285:L250–L257.
27. Cann GM, Guignabert C, Ying L, Deshpande N, Bekker JM, Wang L, Zhou B, Rabinovitch M. Developmental expression of LC3alpha and beta: absence of fibronectin or autophagy phenotype in LC3beta knockout mice. _Dev Dyn_ 2008;237:187–195.
28. Chen ZH, Lam HC, Jin Y, Kim HP, Cao J, Lee SJ, Ifedigbo E, Parameswaran H, Ryter SW, Choi AM. Autophagy protein microtubule-associated protein 1 light chain-3B (LC3B) activates extrinsic apoptosis during cigarette smoke-induced emphysema. _Proc Natl Acad Sci USA_ 2010;107:18880–18885.
29. Pankiv S, Clausen TH, Lamark T, Brech A, Bruun JA, Outzen H, Øvervatn A, Bjørkøy G, Johansen T. p62/SQSTM1 binds directly to Atg8/LC3 to facilitate degradation of ubiquitinated protein aggregates by autophagy. _J Biol Chem_ 2007;282:24131–24145.
30. Yu L, Alva A, Su H, Dutt P, Freundt E, Welsh S, Baehrecke EH, Lenardo MJ. Regulation of an ATG7-beclin 1 program of autophagic cell death by caspase-8. _Science_ 2004;304:1500–1502.
31. Ogata M, Hino S, Saito A, Morikawa K, Kondo S, Kanemoto S, Murakami T, Taniguchi M, Tanii I, Yoshinaga K, et al. Autophagy is activated for cell survival after endoplasmic reticulum stress. _Mol Cell Biol_ 2006;26:9220–9231.
32. Li C, Capan E, Zhao Y, Zhao J, Stolz D, Watkins SC, Jin S, Lu B. Autophagy is induced in CD4+ T cells and important for the growth factor-withdrawal cell death. _J Immunol_ 2006;177:5163–5168.
33. Jia G, Cheng G, Gangahar DM, Agrawal DK. Insulin-like growth factor-1 and TNF-alpha regulate autophagy through c-jun N-terminal kinase and Akt pathways in human atherosclerotic vascular smooth cells. _Immunol Cell Biol_ 2006;84:448–454.